

HUNTINGTON MEDICAL RESEARCH INSTITUTES
NEUROLOGICAL RESEARCH LABORATORY
734 Fairmount Avenue
Pasadena, California 91105

Contract No. NO1-NS-5-2324
QUARTERLY PROGRESS REPORT
October 1 - December 31, 1996

Report No. 8

"SAFE AND EFFECTIVE STIMULATION OF NEURAL TISSUE"

William F. Agnew, Ph.D.
Douglas B. McCreery, Ph.D.
Ted G.H. Yuen, Ph.D.
Randy R. Carter, Ph.D.
Leo A. Bullara, B.A.

This QPR is being sent to
you before it has been
reviewed by the staff of the
Neural Prosthesis Program.

ABSTRACT

During the past quarter we have completed chronic intracortical implants in 6 cats using both 7-electrode arrays of activated iridium microelectrodes and multisite silicon microprobes. These animals have been physiologically evaluated by recordings of access resistance, pyramidal tract evoked potentials and single unit neural activity. Histologic results of the iridium arrays are in progress. Results with the silicon multisite electrodes indicate minimal mechanical injury and no electrically-induced injury of tissues adjacent to sites pulsed with charge densities of $2000 \mu\text{C}/\text{cm}^2$ ($8\text{nC}/\text{phase}$, $5\text{A}/\text{cm}^2$). In the absence of commercially available fine wire (less than $100 \mu\text{m}$ diameter), we have developed etching techniques to reduce $100 \mu\text{m}$ diameter wire to $20\text{-}35 \mu\text{m}$ in diameter. This will allow much smaller surface areas and shafts and hopefully decrease the neural damage in future experiments.

INTRODUCTION

These studies are a portion of our investigations of the limits of safe microstimulation of neurons in the brain, and our investigations of the mechanisms underlying the neural damage and dysfunction that may result from surgical implantation and long-term residence of these electrodes in nervous tissue. The studies are utilizing discrete (activated iridium) microelectrodes and multisite silicon microprobes implanted chronically in the cerebral cortex of cats. In this report, we describe our continuing experience with chronically-implanted, electrically active, multisite silicon arrays and arrays of discrete, activated iridium microelectrodes.

METHODS

The procedure for fabricating the chronically implantable assemblies of multisite silicon microprobes ("Michigan probes") was described in our last report (QPR#11). The arrays have horizontal, integrated silicon cables, 2.5 cm in length. The iridium electrode sites have geometric areas of $400 \mu\text{m}^2$. The tips of the tines are formed by a shallow - diffusion boron etch-stop process, which yields tines with very sharp-edged shanks above the tip, and a very sharp tip. The assembly implanted into

cat IC148 incorporated a short silicone rubber crossbeam attached just proximal to the array, to reduce the tendency of the array to sink into the cortex. This modification proved to be quite effective, as noted below.

The final step in fabrication is to activate the iridium sites by potentiodynamic cycling. To reduce the risk of delamination of the iridium/iridium oxide site during prolonged stimulation, the sites on the present array were activated only to a charge capacity of 25 nC (6 mC/cm²).

The shafts of the discrete iridium microelectrodes are fabricated from segments of annealed iridium wire, 50 μ m in diameter. One end of each shaft is etched electrolytically to a cone with an included angle of 10°, and a final tip radius of curvature of approximately 6 μ m (Blunt tips). A thin wire lead, insulated with Teflon, is micro welded near the other end. The shaft is then insulated with 4 thin coats of Epoxylite electrode varnish, and each layer of insulation is baked using a schedule recommended by the manufacturer. The insulation is removed from the tips by dielectric destruction. The geometric area of the exposed metal tip is then determined from a photomicrograph. The geometric surface areas are 500 \pm 40 μ m². The adherence of the insulation to the shaft at the borders of the facet or exposed cone is assessed by fast cyclic voltammetry which provides a means of separately measuring the real area of the surface that is directly exposed to the solution and also that which is accessible only through a high impedance (a film of saline intruding between the edges of the facet and the insulation, or pinhole leaks in the insulation itself). The individual electrodes are then incorporated into arrays of 7, extending 1.5, 1.7 and 2.0 mm from a superstructure that is cast from Hysol epoxy. The cables are incorporated into a percutaneous connector. The array assemblies are soaked for 4 days in deionized water, then sterilized with ethylene oxide prior to implantation.

Using general anaesthesia and aseptic surgical technique, the arrays are implanted into the postcruciate cortex of young adult cats. The scalp and muscles are reflected in a midline incision, and the cruciate (sensorimotor) cortex is exposed. The frontal air sinus is filled with bone cement. In the case of the multisite silicon arrays, the cable junction box is affixed with bone cement to the parietal bone, lateral and

posterior to the craniectomy defect. The suture suspending the array from the support beam is released, and, using padded forceps, the array of microelectrodes is inserted into the cortex through a small slit in the dura. The silicon cable remains above the dura. A similar procedure is used to implant the arrays of 7 discrete iridium microelectrodes. In the animals described in this report, the dura was not closed over the array.

To assist in the implantation of the recording electrode into the pyramidal tract, a surface stimulating electrode, 1 mm in diameter, is placed on the motor cortex adjacent to the microstimulating array. The surface array can excite a large number of corticospinal neurons, and this induces a large compound action potential (CAP) in the pyramidal tract. The flexible stainless steel pyramidal tract recording electrode is inserted by stereotaxis through a small burr hole over the cerebellum, to a region of the tract in the ventral aspect of the brainstem. Its final position in the ventral brainstem is adjusted until the compound action potential from the pyramidal tract is maximized. The lead to the recording electrode is then secured to the posterior fossa with methyl methacrylate bone cement. We have recently modified the introducer used to implant the pyramidal tract recording electrode. The modifications are intended to improve the alignment of the final segment of the recording electrode and therefore to minimize injury to the ventral brainstem and pyramidal tract. In the most recent animals (IC149 and IC150,) the signals from the pyramidal tract appear to be more stable over time. However, we encountered some difficulties while implanting the new electrodes in the two cats described in this report. After all electrodes are implanted, the sensorimotor cortex is covered with two layers of gelfoam, and the bone defect is sealed with methacrylate bone cement. The cats are placed in an incubator where they are monitored until they have recovered from the anesthesia. They are given appropriate postoperative care, including Bupronorphine for relief of postoperative pain.

The chronically-implanted microelectrodes also allowed recording of the action potentials generated by individual cortical neurons. The signals were recorded by means of an 8-channel system with j-fet head-stages, and digitized into the computer at 25,000 samples/sec. We have begun to use the unitary neural activity as a means of

tracking the migration of the arrays through the cortex, and as a second means of determining the effect of the prolonged stimulation on neuronal excitability.

The prolonged stimulation protocols were conducted 50 or 105 days after implantation of the arrays. Throughout the stimulation, the cats were anesthetized with Propofol. For both types of arrays, the stimulus was biphasic, cathodic-first current pulses, 400 μsec /phase in duration and 20 μA in amplitude (8 nC/phase, 5 A/cm².) The charge density is 2,000 $\mu\text{C}/\text{cm}^2$ in the case of the multisite silicon arrays, and 1,600 $\mu\text{C}/\text{cm}^2$ for the discrete iridium electrodes. The stimulus frequency was 100 Hz.

Within 30 minutes after the end of the 7-hour test stimulation, the cats were perfused for histologic evaluation of the implant sites. A brief saline rinse is perfused through the ascending aorta, followed by 2L of Karnovsky's fixative (3% glutaraldehyde and 2% paraformaldehyde in 0.1 M sodium cacodylate buffer, pH 7.4). This fixative can be used for both light and electron microscopy of brain tissue. Perfusion is effected at 120 mm Hg, using a peristaltic pump (Model #7520-25 Cole-Palmer Instrument Co., Chicago, IL).

Following perfusion, the head with brain and array in situ, is left in fixative until autopsy the following day. At autopsy the overlying tissue is dissected from the arrays, the arrays are removed from the brain and examined with a dissecting microscope for evidence of adherent brain tissue, then stored in glycerin for future scanning electron microscopy of the electrode sites. The array sites in the brain are examined for evidence of hemorrhage, infection, tissue compression and connective tissue formation around the array matrix. In most cases, photographs are taken of the implant sites before and after removal of the arrays.

Tissue samples designated for light microscopy are resected as a single block containing all electrode tracks. Serial paraffin sections are stained with Nissl (for assessment of neural elements), or with Hematoxylin and Eosin (a nuclear stain used to identify the cell types of any inflammatory infiltrates). A few sections are stained with Masson's trichrome, to highlight connective tissue (scars), or with special histochemical stains (for example, for glial fibrillary acidic protein, GFAP). The precise sites of the pulsed and unpulsed tissue was determined by measuring from the electrode tip site to

the active sites using several serial sections.

Special attention is given to the distribution and extent of electrical neural damage adjacent to pulsed sites or due to mechanical factors, and the presence of microvacuoles and microhematomas that arise from injury to the blood vessels of the parenchyma. The microvasculature is examined to determine the extent of neovascularization.

FABRICATION OF IRIIDIUM WIRE ELECTRODES

Small diameter iridium wire (less than 100 μm dia) is no longer commercially available from wire manufacturing companies (Sigmund Cohn Corp., Medwire Corp., The Wilkenson Corp., Johnson Matthey Co., Leico Ind., Inc., H. Cross Co., Englehard Ind., Cooner Wire, California Fine Wire Co., AM Systems, Inc., In Vivo Metric Systems, Goodfellow Corp.). Although small diameter iridium wire (12.7 μm) was available 10 or 15 years ago, manufacturers stopped producing it due to low demand and the production of toxic products in the manufacturing procedures.

HMRI has designed and implemented techniques to reduce the diameter of the commercially available wire from 100 to 125 μm down to 20 to 35 μm , by electrolytic etching. It has been determined that the key factor in obtaining a uniform diameter along the length of the wire is to maintain a nearly constant current amplitude per unit of wire surface area. Inasmuch as the surface area is continually becoming smaller as the diameter decreases, the current must be reduced accordingly. Details of this methodology will be presented in a future progress report.

Fabrication of silicon (Michigan) microelectrodes has been held up this quarter due to malfunction of the Caltech pad bonder. Arrangements have been made for the use of a pad bonder at another Institution.

RESULTS

Table 1 presents the experiments completed and experiments in progress for this quarter.

TABLE 1
INTRACORTICAL MICROELECTRODE IMPLANTS

| IC # | TYPE ELECT. | STIM/UNSTIM* | PHYSIOLOGIC EVALUATION | HISTOLOGIC EVALUATION |
|------|---------------------------|-------------------------------|--|-----------------------------------|
| 147 | Iridium (7 electr.) array | 5 of 7 electrodes | Recorded single unit activity only | Tissue lost (see text) |
| 148 | Silicon (16 sites) | 8 sites functional Stim. 3 | Single unit activity only | Minimal neural damage, all sites. |
| 149 | Iridium (7 electr.) array | Pending | 1) Single unit activity 2) Pyramidal tract activity | Pending |
| 150 | Iridium (7 electr.) array | Pending | 1) Single unit activity 2) Pyramidal tract | Pending |
| 151 | Iridium | Pending | 1) Single unit activity pending 2) Pyramidal tract all 7 electrodes | Pending |

***Stimulus parameters:** Continuous stimulation for 7 hrs. at 20 μ A, 400 μ sec (cathodic first) at a pulse repetition of 100 Hz (8 nC/phase, 5A/cm²). The charge density was 2,000 μ C/cm² for the multisite silicon electrodes and 1,600 μ C/cm² for the discrete iridium electrodes.

IC147. This array of 7 discrete activated iridium microelectrodes was implanted in the postcruciate cortex for 105 days. We experienced two significant technical problems with this animal. Difficulties with the modified pyramidal tract recording electrode precluded the recording tip from being positioned properly in the ventral brainstem. Secondly, the animal's brain was frozen solid after fixation, when the refrigerator's thermostatic control failed. The latter accident precluded histologic evaluation of the implant sites. However, some physiologic data were obtained which was valuable as a basis for evaluating the performance of the multisite silicon arrays.

The stimulation regimen was conducted with the cat anesthetized with Propofol. Five of the seven microelectrodes were pulsed continuously and simultaneously for 7 hours using biphasic current pulses 20 μ A in amplitude, a pulse duration of 400 μ sec/phase, and a pulse repetition rate of 100 Hz. The cat was perfused for histologic evaluation, approximately 30 minutes after the end of the stimulation regimen.

Figure 1A and 1B show single-unit neural activity recorded from microelectrodes #1 and #3 in the postcruciate gyrus, just before the start of the 7 hours of stimulation. Figure 1C shows activity recorded from electrode #3 just after the stimulation regimen. The well-resolved unitary activity shown in Figure 1A probably was from a neuron very

close to the electrode tip; this cell was silent after the 7-hour stimulation regimen. The less well-resolved activity recorded via microelectrode #3 probably originated somewhat farther from the microelectrode tip and was still present after the 7-hour stimulation regimen. The greater distance from the site of stimulation may have afforded these neurons some protection from stimulation-induced depression of neuronal excitability.

Figure 2A is a plot of the access resistance of one of the 5 pulsed microelectrodes throughout the 7-hour stimulation regimen. The behavior was quite consistent across the group of 5 microelectrodes and is typical of iridium microelectrodes with small tip areas ($500\text{ }\mu\text{m}^2$). The access resistance initially increased rapidly from 70 Kohms to 120-130 Kohms. Figure 2B shows the voltage between the microelectrode and the Ag/AgCl reference electrode at the end of the cathodic and anodic phases of the current pulse. If this endphase voltage is excessive, there will be continuous conversion of the iridium metal to iridium oxide during prolonged pulsing, ultimately causing spalling of the oxide and failure of the electrode.

IC148; physiologic results. This 16-site, 4-tine silicon microprobe was implanted in the precruciate gyrus for 50 days. At the time of receipt from the University of Michigan, the integrated cable was damaged and only 8 sites were functional. During the implantation surgery, the cable sustained further damage, and at the end of the procedure, only 4 sites registered electrical continuity. These continued to function well throughout the 50 days in vivo. Figure 3A shows unitary neural activity recorded from one site, just prior to the 7-hour stimulation regimen. The action potentials from 2 or 3 neurons is discernible. The signal-to-noise resolution of one unit is comparable to the best obtained with chronically-implanted discrete iridium microelectrodes (e.g., Figure 1A above). The large unit was silent after the 7-hour stimulation regimen, probably because the cell was very close to the site of stimulation. The good resolution of the unitary activity before stimulation is consistent with the excellent condition of the brain adjacent to the probes, as described in the next section of this report.

Three electrode sites (7, 14 and 15) were pulsed continuously and simultaneously for 7 hours at 20 μ A, 400 μ sec/phase (cathodic first) and at a pulse repetition rate of 100 Hz. Figure 4A-4C show the access resistance of the 3 sites through the 7-hour regimen. The access resistance remained quite constant, in the range of 70-10 Kohms. Interestingly, the access resistance of these sites was slightly lower and less variable than that of the discrete iridium electrodes described in the previous section. The geometric surface area of these electrode sites is slightly less than those on the discrete microelectrodes (400 vs. 500 μ m²), but the geometry of the two type of sites is quite different (rectangular apertures on the side of a planar probe, vs. a blunt cone at the end of the iridium shafts).

Figure 5A-C show the cathodic and anodic end phase voltage transients for the three pulsed electrodes sites. The end phase voltages of two of the sites remained low, and this is consistent with long life during pulsing. The transients across the third site increased to over \pm 3 volts.

IC-148; histologic results. Fig. 6 shows, schematically, where the electrode array was implanted in the left precruciate gyrus, parallel to the long axis of the gyrus. The arrows indicate the 3 electrode sites (out of 16) which were pulsed.

Hemorrhages or cavitations were not encountered. However, small scars representing resolution of earlier hemorrhages near the tips of electrode #'s 2 and 4. The scars were 75 \times 75 μ m and 50 \times 100 μ m in size, respectively.

Occasional neurons near all tracks were mechanically flattened (Figs. 7-10) but appeared otherwise normal. Only occasional lymphocytes were present near the tracks, whether pulsed or unpulsed, and there was no predilection for any of the three pulsed sites on tines 2 or 4 (Fig. 11).

Slight- to- moderate gliosis was present near three of the tracks and, along track #4, extended continuously for 620 μ m, from a depth of 2,320 to 2,940 μ m (Figs. 12,13). Vascular hypertrophy was prominent near the tip of track #4 (Fig. 14).

DISCUSSION

The striking amelioration of mechanically-induced neural injury including microhemorrhages at the sites of silicon multisite electrodes found in this study confirms our previous reports in QPR #5 and #7. This is most encouraging. In addition, the lack of electrically induced injury at the 3 sites pulsed with charge densities of $2,000 \mu\text{m}$ and charge/ph of 8 nC also confirms our previous observations that the cerebral cortex is very resistant to electrically-induced neural damage. The histological results in the single animal presented here do not confirm our previous findings of lymphocyte electrotaxis at pulsed electrode sites. The absence of lymphocytes may be due to the fact that the array had been implanted for 50 days. This phenomenon will be closely followed in the remaining animals of the series, especially with regard to the time of sacrifice following the stimulus regimen.

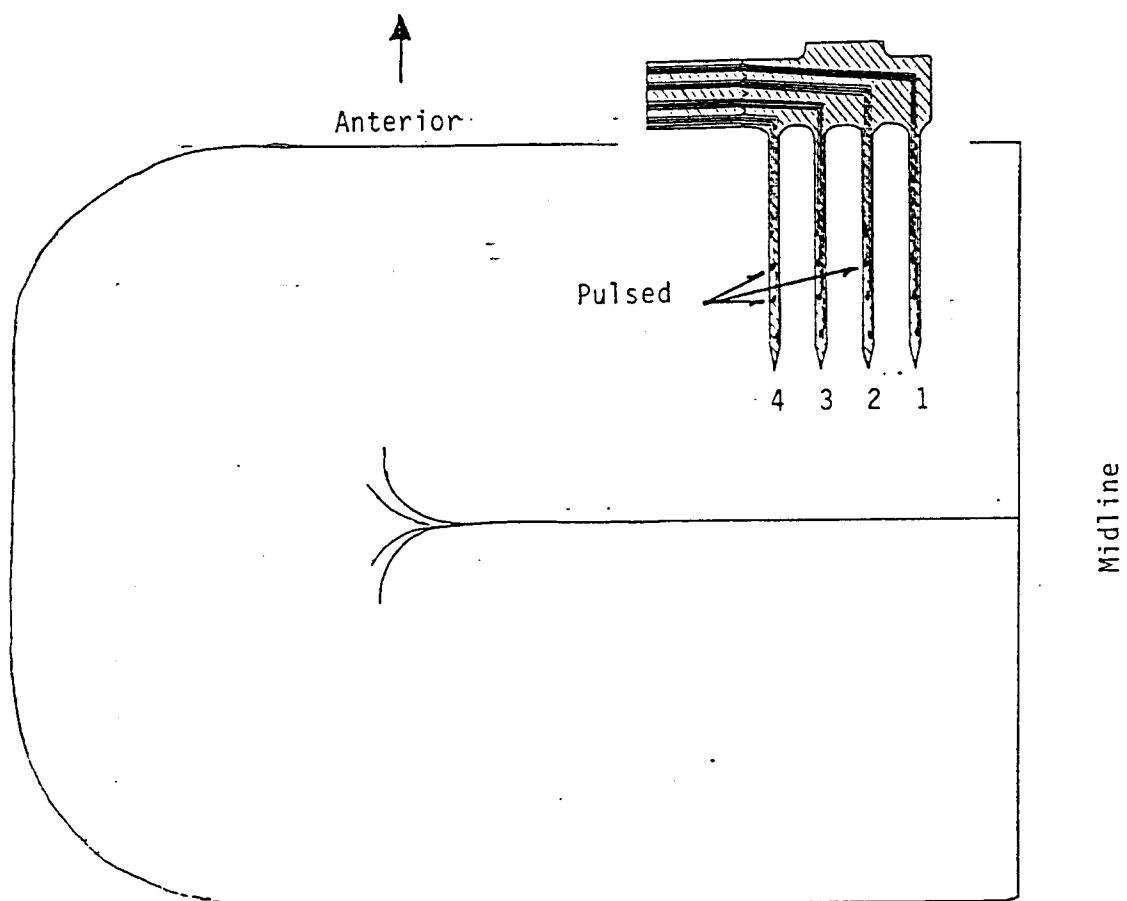
Several factors may contribute to the marked decrease in mechanically-induced neural injury in the use of silicon multisite electrodes. The first is that we are no longer suturing the dura over the implanted arrays. Rather, the dural flaps are approximated and overlaid with moist gelfoam, thus reducing the possibility of electrode movement after implantation. A second possibility for reduced mechanical damage with silicon electrodes compared to discrete iridium electrodes is the much smaller size of the former ($15 \mu\text{m}$ thick and $150 \mu\text{m}$ wide). For this reason, we are optimistic that the reduction of the size of the activated iridium microelectrodes will correspondingly reduce the mechanically-induced injury when they are inserted into the cortex.

The stability of the access resistance of the iridium sites on the silicon probes indicates that the iridium did not delaminate from the underlying titanium during the stimulation regimen, as apparently had occurred previously with some of these probes. This may be due to our modification of the procedure for activating the iridium sites, as described in Methods. The end phase voltages of two of the sites remained low throughout the pulsing regimen and this is consistent with long life during pulsing. The transients across the third site increased to over ± 3 volts. While transients of this magnitude often occur during prolonged pulsing of discrete iridium electrodes (e.g., Fig. 2B), the silicon probes may be less tolerant of prolonged pulsing a high end phase

voltages. The titanium sites on the silicon probes are covered by a rather thin layer of iridium, all of which may eventually be converted to oxide and may spall from the titanium if the end phase potentials reach ± 3 volts. We are continuing to examine the relation between the initial activation schedules and the voltage transients during pulsing in vivo. We also plan to examine the three pulsed sites by scanning electron microscopy, and the findings will be reported in the next QPR.

WORK NEXT QUARTER

We will continue implanting both discrete iridium electrodes (7 microelectrodes/array) and silicon multisite (Michigan) microelectrodes. These and experiments begun last quarter will be evaluated physiologically and histologically. We will utilize both types of electrodes to determine the effects of pulsing closely spaced microelectrodes (mass effect) as compared to those pulsed individually. These experiments will be carried out using iridium electrodes whose surface area has been reduced by 90% compared to those used previously.



TOP VIEW OF LEFT CRUCIATE GYRUS
(IC148)

Fig. 6

12

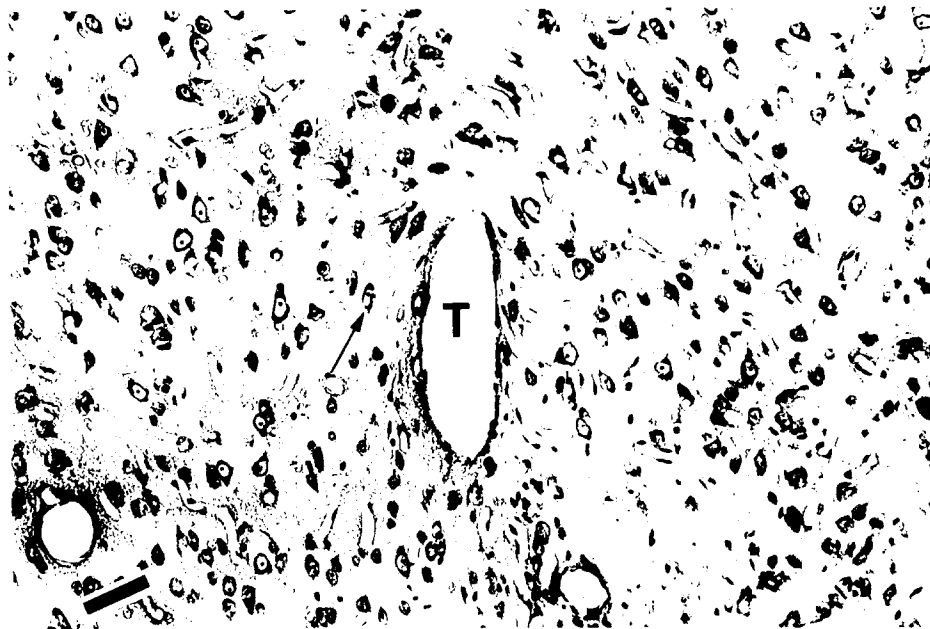


Fig. 7. IC148. Track #1. (Most medial of 4 tracks; all electrode sites unpulsed.) This segment of the track is 1,480 μm deep. An occasional neuron (arrow) is mechanically flattened. However, most of the adjacent neuropil appears normal. Nissl stain. Bar = 50 μm .



Fig. 8. Track #2 (T). Depth = 1,300 μm . Approximate site of the 2nd pulsed electrode site along the probe. Aside from rare, flattened neurons (arrows) and a few glial cells (adjacent to the track) the tissue appears normal. Nissl stain. Bar = 50 μm .

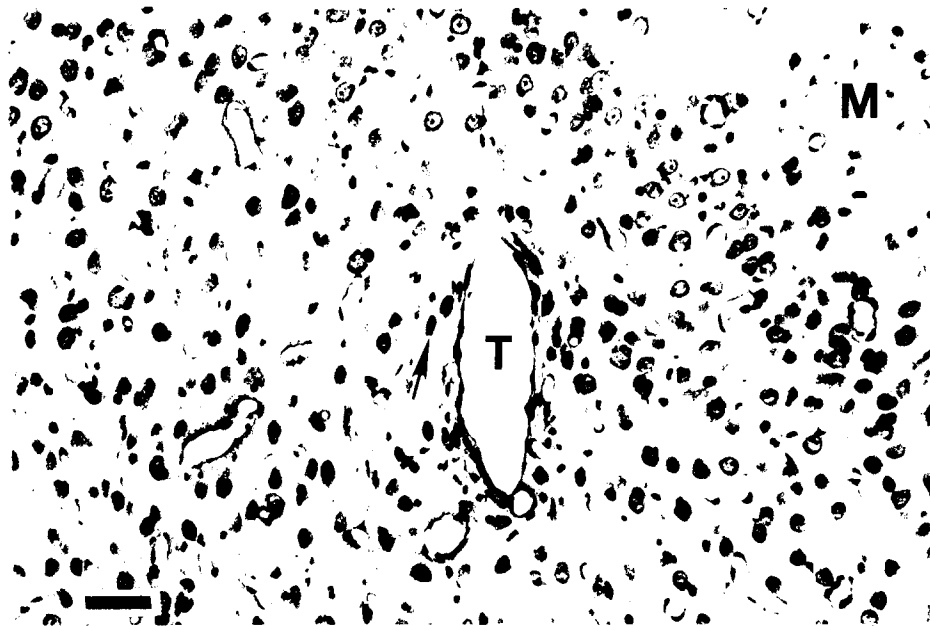


Fig. 9. Track #3 (unpulsed). Depth = 750 μm . This segment of the track lies shallow in the cortex. Although rare neurons are somewhat flattened (arrow) the neuropil appears normal. (M) = molecular layer. Nissl stain. Bar = 50 μm .



Fig. 10. Track #3. The tip of the track (T) is present at a depth of 2,600 μm . This is below most neurons. A few nearby neurons (arrows) are moderately flattened. The dark cells (arrowheads) are presumptive hemosiderophages. Nissl stain. Bar = 25 μm .



Fig. 11. Track #4. Track (T) accompanied by a few glial cells and a hypertrophic blood vessel (V) containing a few lymphocytes (arrows). Nissl stain. Bar = 25 μ m.

Fig. 12. Track #4. This micrograph is taken at a depth of 2,370 μ m. This level is 720 μ m above the electrode tip and is about 80 μ m below a pulsed electrode site. Most cells skirting the track are glia. Lymphocytes are virtually absent. Approximately 620 μ m of the track above the tip was lined by glia. Their location was not correlated with the electrode sites. A few nearby neurons are mechanically flattened (arrows), otherwise the neuropil appears normal. H & E stain. Bar = 25 μ m.

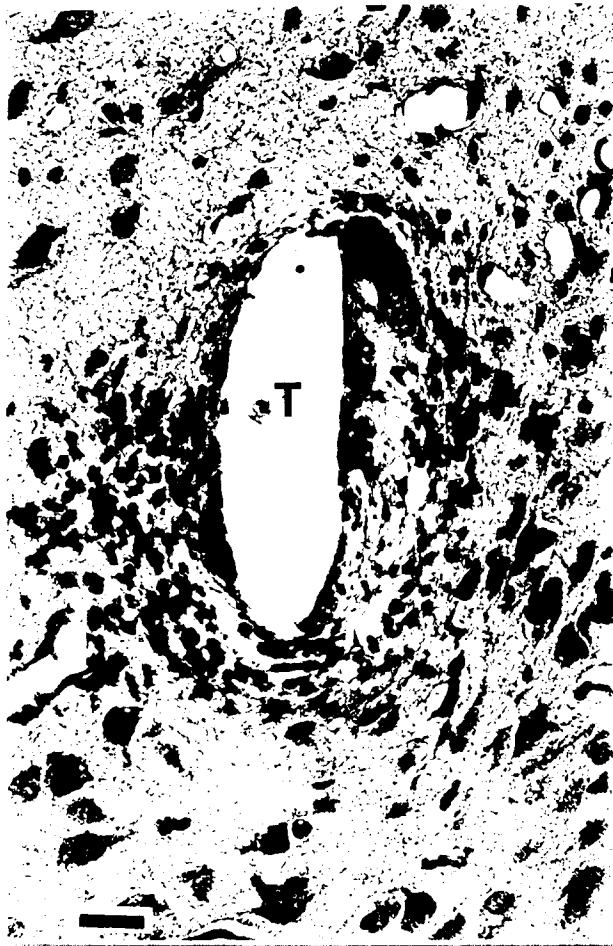


Fig. 13. Track #4. Depth = 2,630 μm . This section is essentially adjacent to the 3rd pulsed electrode. Virtually all of the cells skirting the track are glia with no lymphocytes present. The neuropil appears essentially normal. Nissl stain. Bar = 25 μm .

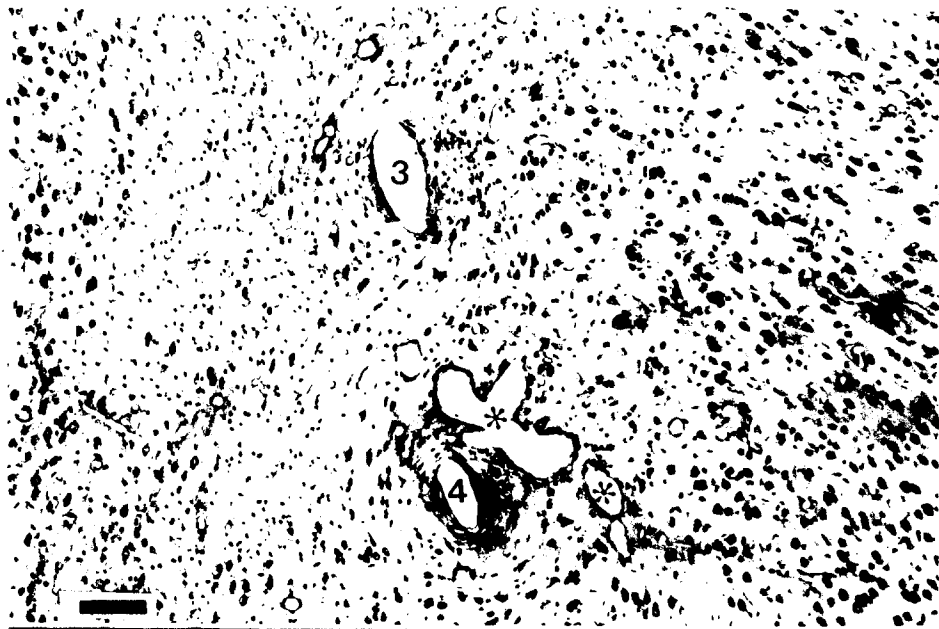


Fig. 14. Depth = 2,840 μm . Tracks #3 (3) and #4 (4) are present. Note the marked vascular hypertrophy(*) near Track #4. At this depth in the cortex, few neurons are present near the tracks. The neuropil adjacent to the tracks appears normal. Nissl stain. Bar = 100 μm .